ELSEVIER

Biophysical Chemistry 107 (2004) 33–49

Biophysical Chemistry

www.elsevier.com/locate/bpc

Complexation of polymethine dyes with human serum albumin: a spectroscopic study

Alexander S. Tatikolov[a,b,*], Sílvia M.B. Costa[a]

[a]*Centro de Química Estrutural, Complexo 1, Instituto Superior Técnico, Av. Rovisco Pais, Lisboa 1049–001, Portugal*
[b]*Institute of Biochemical Physics, Russian Academy of Sciences, ul. Kosygina 4, Moscow 117334, Russia*

Received 30 June 2003; received in revised form 4 August 2003; accepted 4 August 2003

Abstract

Non-covalent interactions between polymethine dyes of various types (cationic and anionic thiacarbocyanines as well as anionic oxonols and tetracyanopolymethines) and human serum albumin (HSA) were studied by means of absorption, fluorescence and circular dichroism (CD) spectroscopies. Complexation with the protein leads to a red shift of the dye absorption spectra and, in most cases, to a growth of the fluorescence quantum yield (Φ_f; for oxonols this growth is very small). The binding constants (K) obtained from changing the absorption spectra and Φ_f vary from 10^4 to $(5–6)\times10^7$ M^{-1}. K for the anionic dyes is much higher than for the cationic dyes (the highest K was found for oxonols). Interaction of *meso*-substituted anionic thiacarbocyanines with HSA results in *cis*→*trans* isomerization and, as a consequence, an appearance and a steep rise of dye fluorescence. Binding to HSA gives rise to dye CD signals and in many cases is accompanied by aggregation of the dyes. These aggregates often exhibit biphasic CD spectra. The aggregates formed by the dyes alone are decomposed in the presence of HSA.

Keywords: Human serum albumin; Polymethine dyes; Complexation; Spectroscopy

1. Introduction

Polymethine (cyanine) dyes have been widely used for probing various organized media (micelles, vesicles, microemulsions, etc.; see, e.g. [1–4]). This is based on their photophysical and photochemical properties, which strongly depend on the nature of the surrounding medium. In particular, fast non-radiative deactivation of cyanines occurs by twisting and rotation of molecular fragments around C–C bonds of a flexible polymethine chain, leading to *trans–cis* photoisomerization and strong dependence of fluorescence lifetimes and quantum yields on the media viscosity [5,6]. Depending on the conditions, cyanine dyes can form aggregates of different types [7]. The labeling of biomacromolecules (in particular, proteins) by cyanines has proven useful: e.g. water-soluble heptamethine cyanine and other near-infra-

*Corresponding author. Tel.: +351-21841-9000; fax: +351-21846-4455.
E-mail address: ast@popsrv.ist.utl.pt (A.S. Tatikolov).

0301-4622/04/$ - see front matter © 2003 Elsevier B.V. All rights reserved.
doi:10.1016/S0301-4622(03)00218-7

red polymethine cyanine dyes can serve as non-covalent labels for the transport blood plasma protein, human serum albumin (HSA) [8,9]; indocyanine green has been used as a diagnostic probe in medical and biological applications [10] and for detection of proteins [11,12]; the infrared cyanine Cy5 has been applied to an immunoassay of HSA [13]; asymmetric and homodimeric monomethine cyanines have been used as fluorescent probes of DNA, RNA and bovine serum albumin (BSA) [14,15]; one of benzothiazolo monomethine cyanine dyes was suggested as a sensitive and specific fluorescent probe for the detection of BSA [16]; some anionic cyanines were proposed for the detection of HSA [17]. Such applications are based on the capability of cyanine dyes for non-covalent interaction (complexation) with biomacromolecules. The main spectroscopic effect upon this interaction is an increase in the fluorescence quantum yield (Φ_f) [10–16,18], which permits using cyanine dyes as fluorescent detectors of biomacromolecules. However, in some cases a drop of Φ_f is observed [19]. Complexation of cyanines with DNA has been investigated in a number of works (see, e.g. [18,20,21]) and can occur by electrostatic binding of the dye to the DNA surface, insertion into the minor groove of double-stranded DNA (often with formation of aggregates) and intercalation into DNA molecule between adjacent base pairs [14,20–22]. At the same time, the interaction of cyanine dyes with proteins has been little studied and the nature of the binding forces and sites is under discussion. A study was reported in the literature where changes in the absorption and fluorescence spectra of some oxadicarbo-, thiadicarbo- and tricarbocyanines were detected in the presence of HSA and other albumins, from which complexation of the dyes with the albumins was deduced [19].

This paper describes a comprehensive spectroscopic study of the main features of the non-covalent interaction between polymethine dyes of various molecular structures and a protein HSA in aqueous solutions by the use of absorption, fluorescence and circular dichroism (CD) spectroscopies. Four classes of polymethine dyes were chosen: (i) cationic thiacarbocyanines (**1**–**4**); (ii) anionic hydrophilic thiacarbocyanines bearing sulfonate groups (**5**–**8**); (iii) anionic oxonols (**9**–**13**); and (iiii) anionic tetracyanopolymethines (**14**, **15**) (see below).

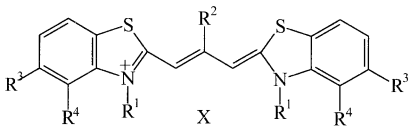

Dye	R^1	R^2	R^3	R^4	X
DTC (**1**)	C_2H_5	H	H	H	I^-
2	$(CH_2)_2OH$	H	H	H	Cl^-
3	$(CH_2)_2OH$	CH_3	H	H	Cl^-
4	n-C_6H_{13}	H	H	H	Br^-
5	$(CH_2)_3SO_3^-$	H	H	H	$C_5H_5NH^+$
6	$(CH_2)_3SO_3^-$	C_2H_5	OCH_3	H	$C_5H_5NH^+$
7	$(CH_2)_3SO_3^-$	C_2H_5	–CH=CH–CH=CH–		$C_5H_5NH^+$
8	$(CH_2)_3SO_3^-$	NH_2	H	H	NH_4^+

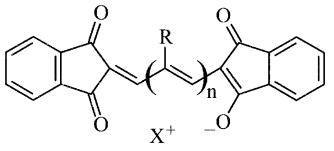

Dye	R	n	X^+
9	H	1	K^+
10	F	1	$(CH_3)_2NH_2^+$
11	CH_3	1	K^+
12	H	2	$(C_2H_5)_3NH^+$
13	H	0	K^+

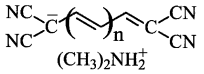

n = 1 (**14**), 2 (**15**).

2. Experimental

2.1. Materials

HSA fraction V, 96–99% purity (catalogue no. A-1653) was purchased from Sigma and used without further purification. Cationic cyanines **1**–**4** were obtained from the dye collection of the Laboratory of Photosensitization (Institute of Biochemical Physics, Russian Academy of Sciences), anionic cyanines **5**–**8** from the dye collection of the Research and Design Institute for the Chemicophotographic Industry (Moscow, Russia) and anionic dyes **9**–**15** from the dye collection of Zh.A. Krasnaya (Institute of Organic Chemistry, Russian Academy of Sciences). Their purity was checked by thin layer chromatography.

Fresh stock aqueous dye solutions, which were kept in a refrigerator in the dark, were used. Phosphate buffer solutions of adequate pH (6.95 or 4.55), NaH_2PO_4, Na_2HPO_4 and NaCl of analytical grade were used as received. Doubly distilled water was used as a solvent.

2.2. Methods

The pH values were measured with a Crison Microph 2002 calibrated using standard buffer solutions. Absorption spectra were recorded with a JASCO V-560 UV–VIS absorption spectrophotometer and fluorescence emission and excitation measurements on a Perkin-Elmer LS 50B spectrofluorimeter, in 1 cm cells, with the sample holders thermostated at 298 K. Corrected fluorescence spectra were obtained using the correction file provided by the manufacturer. Fluorescence quantum yields Φ_f were measured at 298 K using 3,3′-diethylthiacarbocyanine iodide (DTC) in methanol ($\Phi_f = 0.048$ [23]) and rhodamine 101 in ethanol ($\Phi_f = 0.92$ [24]) as standards, after applying the necessary corrections for the refractive index of the solvent. Dye concentrations in fluorescence measurements were approximately 10^{-6} M and below in order to keep the optical density below 0.1. The error in the estimation of Φ_f was $\pm 10\%$.

CD spectra were obtained with a JASCO J-720 spectropolarimeter, in 1 cm quartz cell, with spectral averaging over four spectra and baseline correction, at a constant dye concentration and various protein concentrations [25].

2.3. Data analysis

Interaction of the dyes with HSA was studied by titration of dye solutions with HSA, with a fixed dye concentration and variable [HSA]. The titration was monitored by following the changes in absorbance and fluorescence of the dye. The protein concentration was increased from zero up to the high limiting values until changes in the dye absorbance (or Φ_f) became insignificant. The dye absorption spectrum and Φ_f at such [HSA] were taken as those belonging to the bound dye. We assume here the simple equilibrium between the free (Dye_f) and the bound (Dye_b) dye

$$Dye_f + HSA \overset{K}{\rightleftharpoons} Dye_b \quad (1)$$

with the association constant

$$K = \frac{[Dye_b]}{[Dye_f][HSA_f]}, \quad (2)$$

where $[HSA_f]$ is the concentration of uncomplexed HSA or assuming n non-interacting independent binding sites in HSA,

$$K = \frac{[Dye_b]}{[Dye_f]n[HSA_f]} \quad (3)$$

The solution of the quadratic equation for $[Dye_b]$ gives

$$[Dye_b] = (C + 1/K)/2 - \{(C + 1/K)^2/4 - n[HSA]_0[Dye]_0\}^{1/2} \quad (4)$$

where $C = n[HSA]_0 + [Dye]_0$; $[HSA]_0$ and $[Dye]_0$ $(= [Dye_b] + [Dye_f])$ are the total concentrations of HSA and the dye, respectively. K and n were determined from the computer fit of the $[Dye_b]/[Dye_f]$ values calculated from Eq. (4) to those found experimentally at different [HSA]. The experimental concentrations $[Dye_b]$ and $[Dye_f]$ at each [HSA] were obtained from the computer modeling of the measured absorption spectra as a sum of the spectra of Dye_b (measured at high [HSA]) and Dye_f (measured at $[HSA] = 0$).

Alternatively, K and n were found from the simulation of the experimental Φ_f at different [HSA] by those obtained from Eq. (5):

$$\Phi_f = (\Phi_{ff}\varepsilon_f[Dye_f] + \Phi_{fb}\varepsilon_b[Dye_b])/(\varepsilon_f[Dye_f] + \varepsilon_b[Dye_b]), \quad (5)$$

where Φ_f, ε_f, Φ_{fb} and ε_b are fluorescence quantum yields and extinction coefficients (at the excitation wavelength) of the free and the bound dye, respectively, and $[Dye_b]$ and $[Dye_f]$ were calculated from Eq. (4) ($[Dye_f] = [Dye]_0 - [Dye_b]$). The higher K, the lower dye concentration was used for its determination (at $K \geq 10^7$ M^{-1} [Dye] approx. 10^{-7} M), in order to increase its accuracy (typically approx. $\pm 20\%$).

Usually the application of the Scatchard equations [26]

$$[Dye_b]/([Dye_f][HSA]) = nK - K[Dye_b]/[HSA] \quad (6)$$

or

$$[Dye_b]/[HSA] = n_1K_1[Dye_f]/(1 + K_1[Dye_f]) + n_2K_2[Dye_f]/(1 + K_2[Dye_f]) \quad (7)$$

for obtaining K and n did not give good results due to high scattering of the experimental points. However, Eq. (7) was successfully applied for binding of dye **9** by HSA (see below).

3. Results

3.1. Cationic thiacarbocyanines

3,3′-Diethylthiacarbocyanine iodide (DTC) in water (concentration approx. 10^{-6} M) has the visible absorption band with the maximum at 552.5 nm (Fig. 1a, curve a). Addition of HSA to the solution leads to an initial drop of this band, followed by (at higher HSA concentrations) a gradual red shift and an increase of its intensity up to about the initial value (Fig. 1a, curves b–i). The fluorescence is red shifted and its quantum yield grows (Fig. 1b). Since there are no isosbestic points in the absorption spectra, we may infer that the equilibrium between the free and the bound dye is not simple (there are probably several bound forms of the dye) and it is troublesome to obtain the association constant K from the absorption spectra. However, it appears to be possible to determine the effective association constant K_{eff} from the evolution of Φ_f upon complexation assuming the simple equilibrium between the free and the bound dye (Eq. (1)) (see Fig. 1b). Addition of a neutral phosphate buffer to the solution (0.01 M, pH 6.95) decreases K_{eff} (Table 1). Similar spectroscopic features are inherent in the interaction of DTC structural analogs, thiacarbocyanines **2** and **3**, with HSA (Fig. 1b). The corresponding values of K_{eff} obtained from growing Φ_f in the presence of HSA are listed in Table 1.

Thiacarbocyanine **4** with longer *N*-alkyl substituents has a strong tendency to form aggregates in aqueous solution. The aggregates are non-fluorescent and have a broad absorption spectrum (Fig. 2, curve a; the fluorescence excitation spectrum *f* corresponds to the monomeric dye present in the

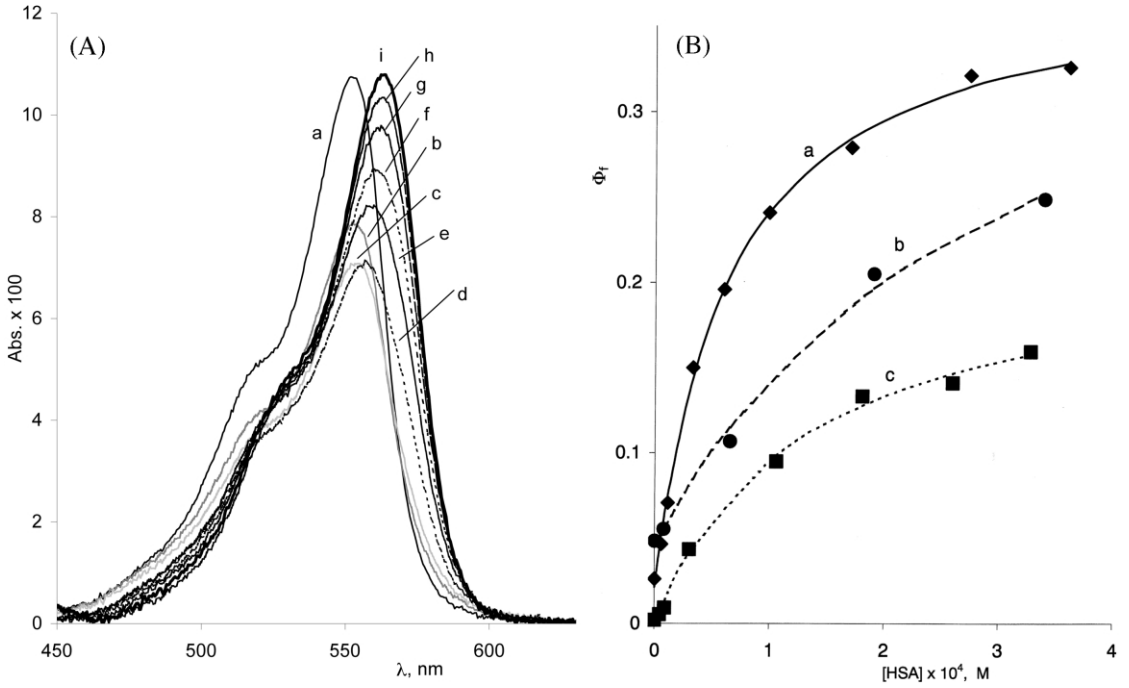

Fig. 1. (A) Absorption spectra of DTC (1.2×10^{-6} M) in aqueous solution in the presence of increasing HSA concentrations: 0 (a); 5.8×10^{-6} (b); 1.14×10^{-5} (c); 3.28×10^{-5} (d); 6.02×10^{-5} (e); 9.93×10^{-5} (f); 1.71×10^{-4} (g); 2.75×10^{-4} (h); and 3.62×10^{-4} M (i). (B) Dependence of the fluorescence quantum yields of DTC (a), **2** (b) and **3** (c) in water on HSA concentration (points) and its approximation based on Eq. (5) (curves) assuming $K=1.74\times10^{4}$ M^{-1}, 3.5×10^{3} M^{-1} and 1.0×10^{4} M^{-1}, respectively, ($n=1$).

system in small amount). Addition of HSA leads to decomposition of the aggregates into the monomeric dye complexed with HSA, which has the absorption spectrum shifted to the red as compared with the free dye (Fig. 2, curves b–e), and is accompanied by enhancement of the fluorescence.

While free cationic thiacarbocyanines (like other polymethine dyes studied here) as symmetric molecules exhibit no CD signals, their complexes with HSA give rise to low-intense negative CD spectra. For example, for DTC (1.5×10^{-6} M) in the presence of HSA (2.2×10^{-4} M) the amplitude of the CD band is approximately 0.10–0.15 mdeg.

3.2. Anionic thiacarbocyanines with sulfonate groups

Addition of HSA to an aqueous solution of **5** results in a drop of the initial absorption band of the free dye ($\lambda_{abs}^{max}=557$ nm) and growing a red-shifted band of the dye bound to HSA ($\lambda_{abs}^{max}=566$ nm). Simultaneously, a strong increase in the fluorescence quantum yield is observed (from 0.05 to 0.68), which also indicates complexation of the dye with HSA. Unlike cationic thiacarbocyanines, an isosbestic point occurs in the absorption spectra.

While **5** is present at moderate concentrations in aqueous solutions in monomeric form, **6** and **7** are in equilibrium with their dimers (and, at higher concentrations, with H aggregates) absorbing in the short-wavelength region (**7** also forms J aggregates absorbing in the red) [27,28]. Upon addition of HSA, the dimeric and aggregate bands are reduced and replaced by the new one (apparently the band of the monomeric dye complexed with HSA). This is accompanied by an appearance and a growth of fluorescence, which is absent in aqueous solutions of **6** and **7** without HSA. For the monomer of dye **6** the binding constant K could be estimated only at sufficiently low con-

Table 1
Association parameters for binding polymethine dyes to HSA

Dye	Buffer	Absorption maxima, nm		K, M^{-1}	n
		Free dye	Bound dye		
1 (DTC)	no	552.5	~565	1.74×10^4 [a]	1.0[a]
1 (DTC)	0.01 M pH 6.95			1.05×10^4 [a]	1.0[a]
2	no	557	~567	3.5×10^3 [a]	1.0[a]
3	no	542	~563	1.0×10^4 [a]	1.0[a]
4	no	broad	565	–	–
5	no	557	566	$(2–3)\times10^6$ [b]	0.03–0.06[b]
				$(8–9)\times10^4$ [b,c]	1.0[b]
6	0.01 M pH 6.95	559	590	1.05×10^7 [b]	0.25[b]
				$\sim1.7\times10^6$ [b,c]	1.0[b]
6	0.01 M pH 4.55			5×10^7 [b]	0.13[b]
				$\sim8\times10^5$ [b,c]	1.0[b]
7	0.01 M pH 6.95	539, 570sh	611	$>10^6$ [a]	(1)[a]
9	no	548	558	6.0×10^7 [b]	1.75[b]
				$K_1=5.5\times10^7$ [d]	1.0[d]
				$K_2=3\times10^7$ [d]	1.0[d]
9	0.01 M pH 6.95			6.0×10^7 [b]	1.03[b]
9	0.1 M NaCl			3.2×10^7 [b]	1.12[b]
10	no	562	574	4.9×10^7 [b]	1.0[b]
10	0.01 M pH 6.95			5.0×10^7 [b]	1.0[b]
12	no	647	662.5	–	–
13	no	455	462	1.5×10^7 [b]	1.0[b]
14	no	437	445	1.9×10^7 [b]	0.75[b]
				$\sim1\times10^7$ [b,c]	1.0[b]
15	no	536	546	5.0×10^7 [b]	0.63[b]
				$\sim1.3\times10^7$ [b,c]	1.0[b]
15	0.01 M pH 6.95			4.8×10^6 [b]	5.3[b]

[a]Found from growing Φ_f.
[b]Found from the evolution of the absorption spectrum using the plot $[Dye_b]/[Dye_f]$ vs. [HSA].
[c]Rough estimate assuming $n=1$.
[d]Found from the evolution of the absorption spectrum using the Scatchard equation.

centrations (approx. 3×10^{-7} M), at which the monomer⇄dimer equilibrium is shifted to the monomer and with HSA an isosbestic point is present in the absorption spectra (Fig. 3a).

It is noteworthy that for dyes **5** and **6** the simulation of the experimental plots $[Dye_b]/[Dye_f]$ vs. [HSA] based on the evolution of the absorption spectra reveals the unrealistic apparent association numbers n much less than unity (Table 1). The simulation of Φ_f dependence on [HSA] as well as the Scatchard plots also give similar values of n. This might be due to occurrence, apart from the simple complexation, partial aggregation of the dyes on HSA at relatively low HSA concentrations:

$$\mathrm{Dye\ HSA + Dye \rightleftarrows Dye_2\ HSA}$$
$$\mathrm{Dye_2\ HSA + Dye \rightleftarrows Dye_3\ HSA}$$

etc.

$$\mathrm{Dye_{\mathit{m}-1}\ HSA + Dye \rightleftarrows Dye_{\mathit{m}}\ HSA} \quad (8)$$

and their deaggregation at higher concentrations of the protein:

$$\mathrm{Dye_{\mathit{m}}\ HSA + HSA \leftrightarrows Dye_{\mathit{m}-1}\ HSA + Dye\ HSA}$$

etc.

$$\mathrm{Dye_2\ HSA + HSA \rightleftarrows Dye\ HSA + Dye\ HSA}, \quad (9)$$

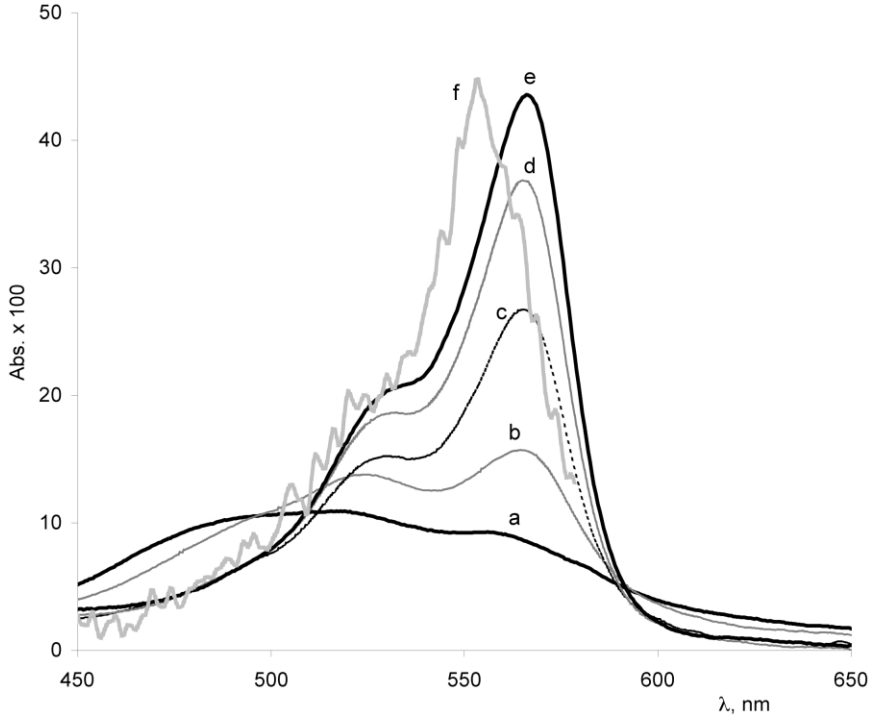

Fig. 2. Absorption spectra of dye **4** (4.4×10^{-6} M) in water as a function of HSA concentration: [HSA] = 0 (a); 3.12×10^{-6} (b); 1.77×10^{-5} (c); 4.3×10^{-5} (d); and 8.0×10^{-5} M (e); fluorescence excitation spectrum at [HSA] = 0 (λ_f = 600 nm) (f).

where m is the aggregation number. Dye aggregates are usually non-fluorescent and often have low extinction coefficients; their formation could result in diminishing the monomeric (bound) dye band and Φ_f at low [HSA], whereas deaggregation of the dyes at higher [HSA] recovers the bound monomeric dye in the system, leading to a curvature of the $[Dye_b]/[Dye_f]$ dependence on [HSA] greater than that without aggregation–deaggregation phenomena and hence to the anomalously low values of n (Fig. 4). In Table 1, along with the apparent K and n obtained from the best fit to the experimental points, the K values roughly estimated from the experimental data assuming $n = 1$ are presented.

Dye 7 even at concentrations as low as 10^{-7} M exists mainly as a dimer [28], so it is impossible to obtain directly the binding constant for its monomer. The estimate made from the evolution of Φ_f gives $K > 10^6$ M^{-1}.

Incorporation of HSA in aqueous solution of dye **8**, apart from the usual effects of the red shift of the absorption spectrum and growing fluorescence, results in the appearance of a long-wavelength absorption shoulder ($\lambda_{max} \approx 545$ nm). Since this new species possesses fluorescence with rather small Stokes shift (approx. 12 nm; see Fig. 5), it may be reasonable to suppose that it is a J aggregate of the dye formed on HSA. Interestingly, we did not find any J aggregation of dye **8** alone in aqueous solutions.

Complexation of dyes **5**–**7** with HSA results in appearance of CD spectrum in the wavelength region of the dye absorption spectrum, which has negative sign (for dye **6** see Fig. 3b). For dye **5** (2×10^{-6} M) its amplitude is approximately 0.3 mdeg at $[HSA] = (0.7-1.0)\times10^{-4}$ M.

3.3. Anionic oxonols

Oxonols belong to the class of anionic polymethine dyes with negative charge shared among four

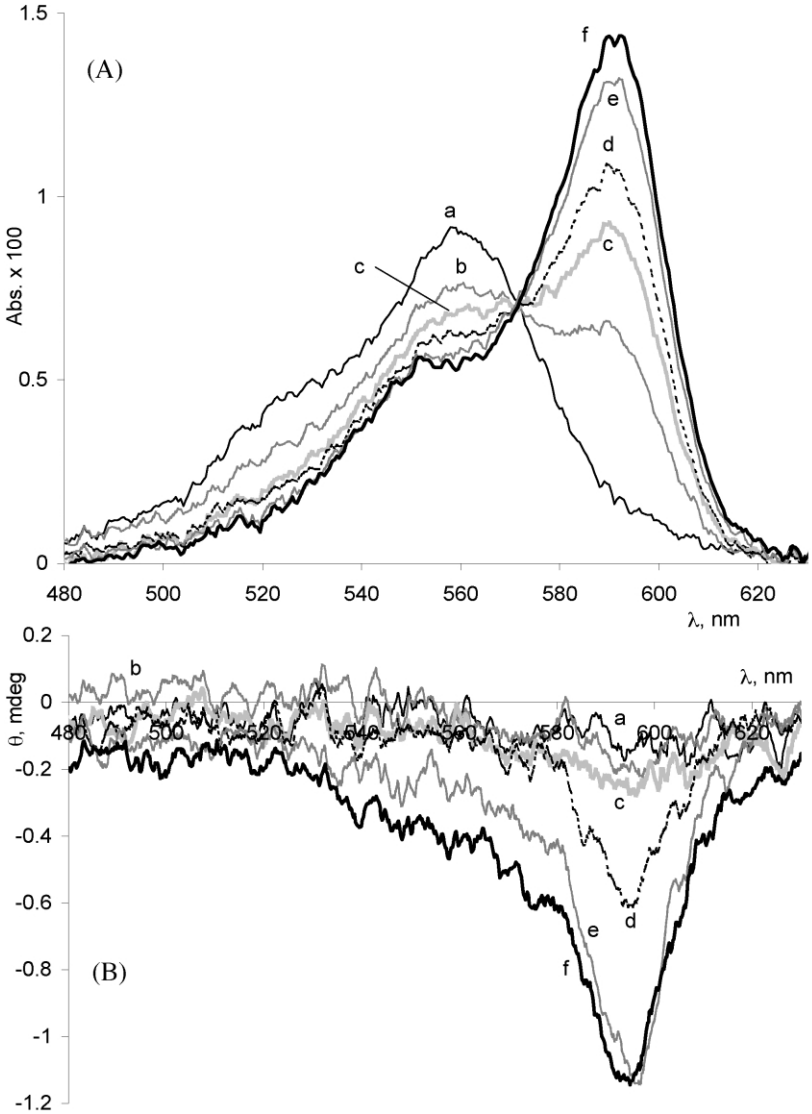

Fig. 3. (A) Dependence of the absorption spectrum of dye **6** (1.46×10^{-7} M) on HSA concentration in 0.01 M phosphate buffer pH 6.95: [HSA] = 0 (a); 5.0×10^{-7} (b); 1.0×10^{-6} (c); 2.0×10^{-6} (d); 3.0×10^{-6} (e) and 4.9×10^{-6} M (f). (B) CD spectra of dye **6** (1.7×10^{-6} M) with HSA in 0.01 M phosphate buffer pH 6.95. [HSA] = 1.0×10^{-7} (a); 2.0×10^{-7} (b); 5.0×10^{-7} (c); 1.0×10^{-6} (d); 2.0×10^{-6} (e) and 5.0×10^{-6} M (f).

oxygen atoms. They are rather stable in aqueous solutions and have absorption spectra similar to those of thiacyanines with the polymethine chain of the same length. Oxonols 9–13 are non-fluorescent in water. Incorporation of HSA into aqueous solutions of **9**–**13** results, as usual, in the decrease of the initial monomeric band of the free dye and growing of the red-shifted band of the dye bound to HSA, for **9**, **10** and **13** with the presence of an isosbestic point in the spectra. The binding constants obtained from the evolution of the absorption spectra are very high ($>10^7$ M^{-1}; see Table 1). However, unlike cyanines, the fluorescence growing upon the complexation is very small (at

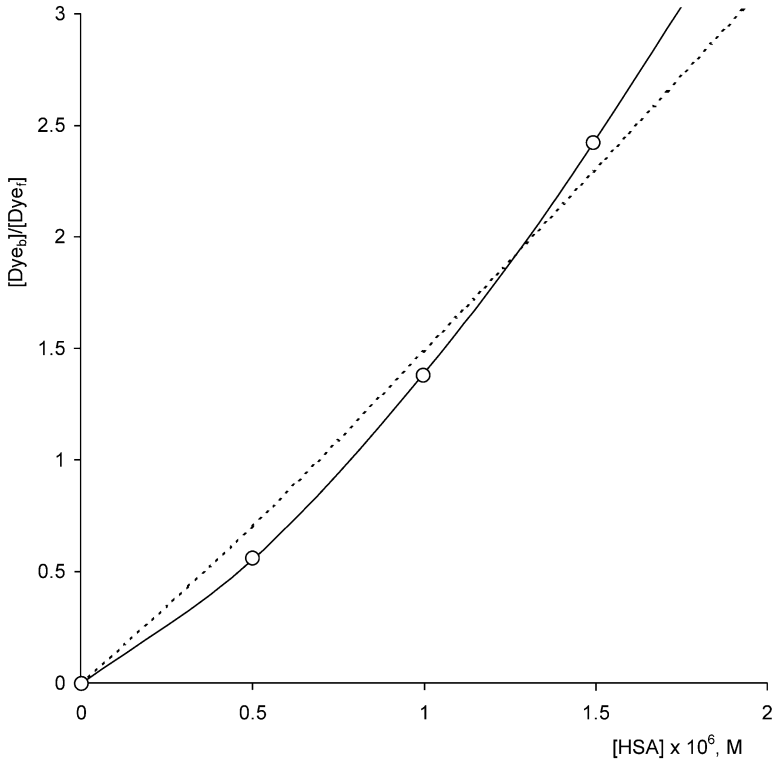

Fig. 4. Experimental plot $[Dye_b]/[Dye_f]$ vs. [HSA] for dye **6** obtained from the evolution of the absorption spectrum (circles) and its simulation using $K=1.05\times10^7$ M^{-1}, $n=0.25$ (solid line) and using $K=1.7\times10^6$ M^{-1}, $n=1$ (dashed line).

$[HSA]=(1.8–2.0)\times10^{-6}$ M $\Phi_f=1.2\times10^{-3}$, 4.8×10^{-4} and 5×10^{-3} for **9**, **10** and **12**, respectively). The association number n found for **9** using Eq. (4) is larger than 1 (for **10** and **13,** $n=1$) (Table 1). Simulation of the interaction in terms of the Scatchard Eq. (7) gives for 9 two complexation constants close to each other. This means that **9** binds to HSA in two sites (two dye molecules per one HSA), whereas bulkier dye **10** binds in a single site. Unlike other oxonols, the fluorescence spectrum of **9** bound to HSA is broad (Fig. 6), probably because of the contribution of two bound dye species to the emission. An increase in the ionic strength of the solution by addition of 0.01 M neutral phosphate buffer (pH 6.95) decreases n for **9** down to 1 (only one binding site remains), having minor effect on K. Furthermore, increase in the ionic strength (by introducing 0.1 M NaCl) decreases K (see Table 1). Hence, one of the two HSA sites binding **9** (with lower K) is more sensitive to the ionic strength and, therefore, its binding affinity is of higher electrostatic character. In the presence of acidic buffer (0.01 M, pH 4.55) the isosbestic point in the absorption spectra of **9** and **10** with HSA is lost. This is due to aggregation–deaggregation of the dye on positively charged HSA expressed by Eqs. (8) and (9). The complexation is accompanied by the appearance of a positive band in the CD spectrum (Fig. 7a). Aggregation of **9** on HSA at low pH is confirmed by the change of the CD signal shape, which is biphasic (a couple of positive and negative bands) at relatively small HSA concentrations ($(1–3)\times10^{-7}$ M) when the aggregation takes place, and transforms into the uniform (positive) band at higher [HSA] when the aggregates decompose into the bound monomer (Fig. 7b). While the uniform CD band can be produced by the

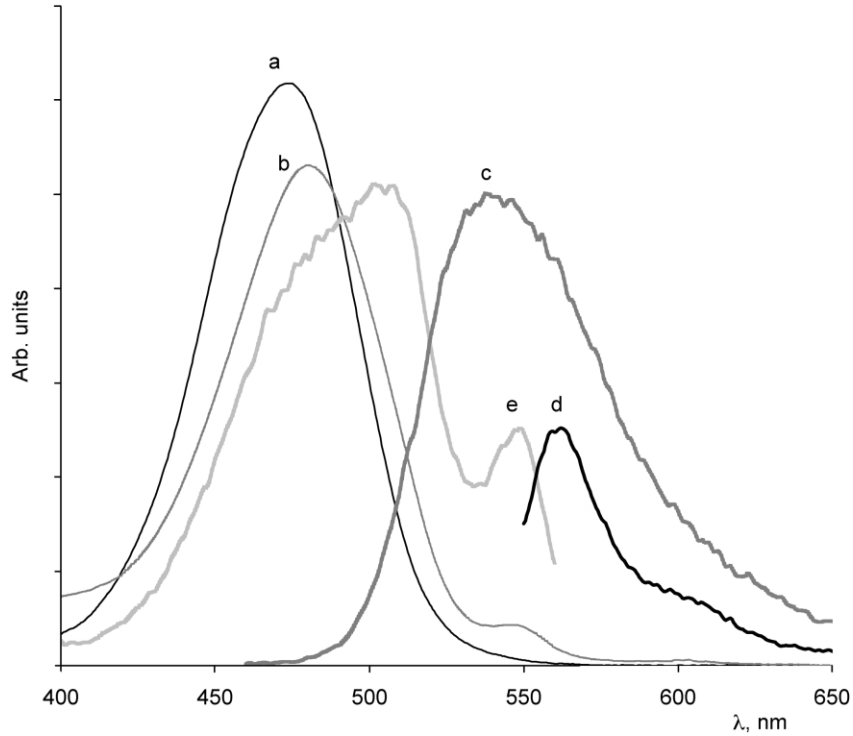

Fig. 5. Absorption spectra of dye **8** (5.8×10^{-6} M) in water at [HSA] = 0 (a) and 5.0×10^{-5} M (b) as well as fluorescence emission (c, d) and excitation (e) spectra of **8** with HSA (5.0×10^{-5} M). λ_{ex} = 450 nm and 540 nm for c and d, respectively; for e λ_f = 570 nm.

monomeric dye molecules, the biphasic CD spectra are known to characterize dye aggregates on biomacromolecules (as a result of exciton coupling of the adjacent dye molecules) [20,21,29]. A comparison of the wavelengths of the biphasic CD spectrum with those of the dye absorption spectrum shows that the aggregate and the monomer spectra lie in similar wavelength regions.

Dyes **11** and **12** in the presence of HSA exhibit no isosbestic points in their absorption spectra apparently due to partial aggregation of the dyes on HSA. Greater ability of these dyes for aggregation could be the consequence of their higher hydrophobicity.

3.4. Anionic tetracyanopolymethines

Tetracyanopolymethine dyes possess the simple structure with formal negative charge on two terminal carbon atoms of the polymethine chain. Upon addition of HSA, the absorption bands of tetracyanopolymethines **14** and **15** in water transform into the red-shifted ones having lower extinction coefficient (with an isosbestic point in the absorption spectra), which belong to the dyes complexed with HSA (Fig. 8a). Simultaneously a moderate rise of Φ_f is observed (for **15** from 0.029 to 0.12). For both dyes the complexation constants K found from changing the absorption spectra are of the order of 10^7 M^{-1} (Table 1). The apparent association numbers n found from the best fit to the experimental plots $[Dye_b]/[Dye_f]$ vs. [HSA] are less than 1, probably due to aggregation–deaggregation phenomena. This is confirmed by the evolution of the CD spectrum of **15** with growing [HSA]. CD appears as biphasic (negative–positive) aggregate spectrum (in the same wavelength region as the absorption band) at

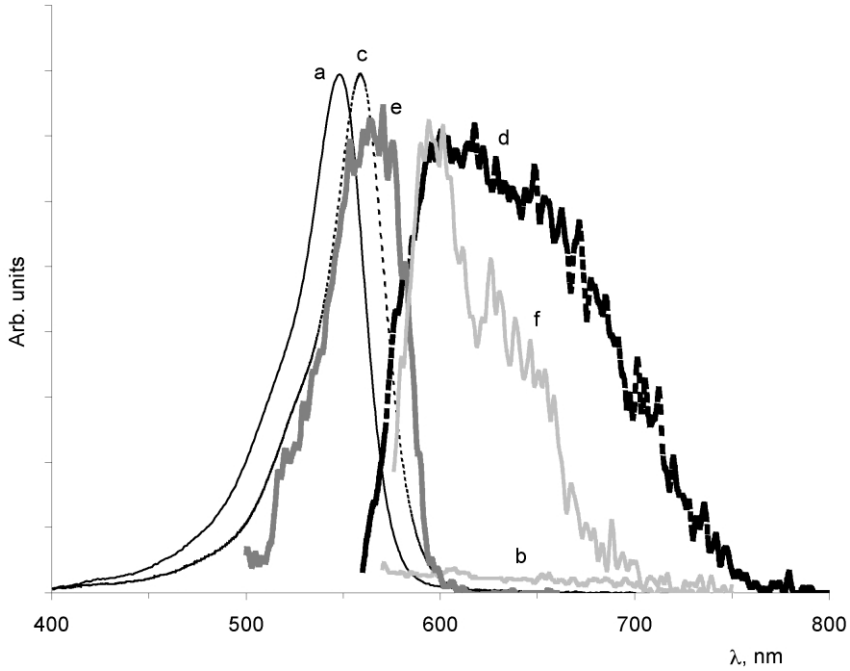

Fig. 6. Absorption (a) and fluorescence (b) spectra of dye **9** (1.5×10^{-6} M) in water; the same in the presence of 2.0×10^{-6} M HSA (c and d, respectively); fluorescence excitation spectrum of **9** in the presence of HSA ($\lambda_f=680$ nm) (e). For comparison, fluorescence spectrum of **10** in the presence of 1.8×10^{-6} M HSA (f) ($\lambda_{ex}=550$ nm).

moderate HSA concentrations ($(1–7)\times10^{-6}$ M) and completely disappears at higher [HSA] (Fig. 8b). At low pH the isosbestic point in the spectra of **15** is blurred out; in the presence of 0.01 M phosphate buffer pH 4.55 the association number *n* estimated from the changes in the absorption spectrum was found to be 5.3 (Table 1). This points to essential aggregation of the dye on HSA with the average aggregation number 5.3 and the aggregate absorption band slightly shifted to the red, the deaggregation process being insignificant in the HSA concentration range studied ($(0-3.4)\times10^{-7}$ M).

4. Discussion

The experimental data show that polymethine dyes can bind non-covalently to HSA with the association constants ranging from 10^4 to $(5–6)\times10^7$ M^{-1}. Since HSA at neutral pH has overall negative charge (its $pK_a\approx5.4$ [30]), we might expect at pH 7 the highest binding affinity for oppositely charged cationic thiacarbocyanines. However, they exhibit the lowest *K* (approx. 10^4 M^{-1}), which is much higher for the anionic dyes (Table 1). Analogous behavior was found earlier for porphyrins: the positively charged compounds showed no evidence of binding to HSA, while negative porphyrins did [29,31]. Similarly, ochratoxin A binds strongly to HSA only in its dianionic form [32]. Therefore, we may infer that the overall HSA charge does not play a crucial role in binding dyes, and different local charges of binding sites are of importance. It can be seen from the data of Table 1 that for cationic thiacarbocyanines **1**–**3** (i) a rise of ionic strength of the solution (by addition of a neutral buffer) decreases *K*; (ii) incorporation of hydrophilic groups (OH) into the dye molecule decreases *K* (cf. DTC and **2**); and (iii) hydrophobic substituents (CH_3) in the dye increase *K* (cf. dyes **2** and **3**). Hence, we may conclude that both electrostatic and hydrophobic forces are operative upon complexation of these dyes with HSA. A rise of Φ_f is observed apparently due to hindering intramolecular motions of dye molecules in restricted environment of the binding sites and a

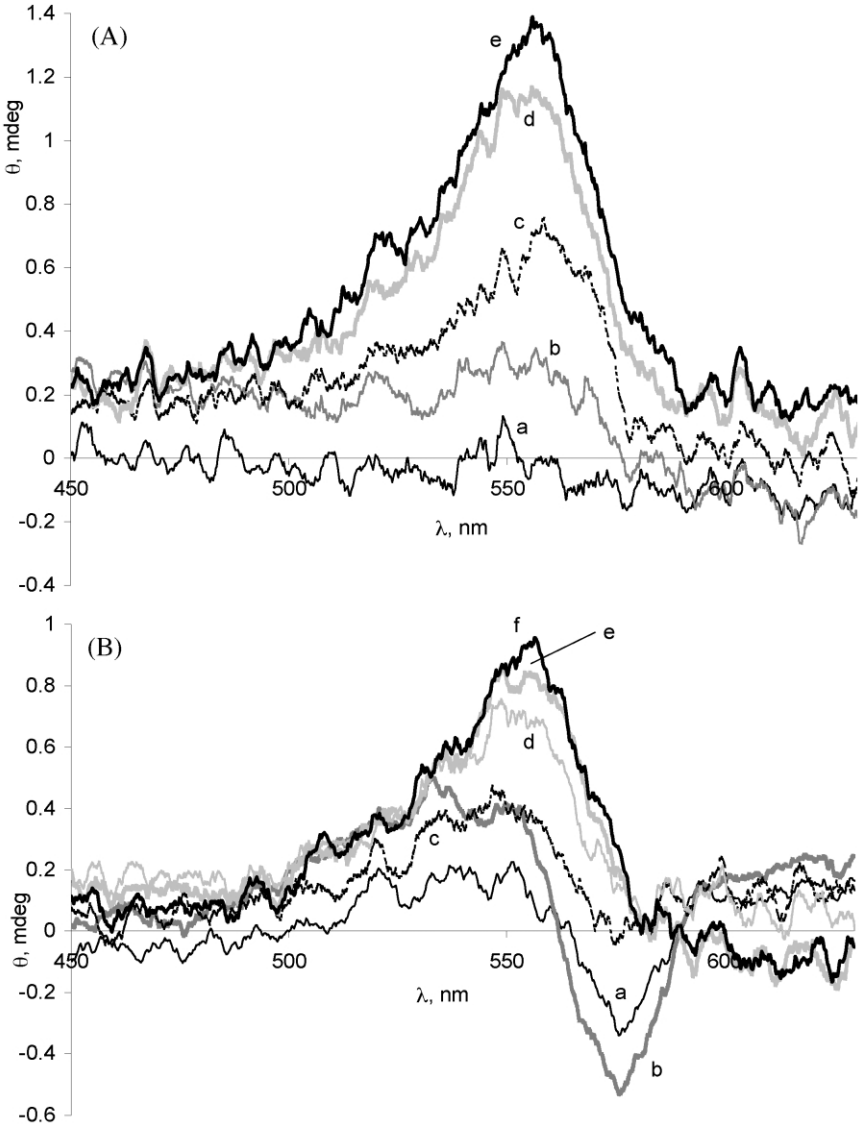

Fig. 7. (A) CD spectra of dye **9** (2.0×10^{-6} M) with HSA in 0.01 M phosphate buffer pH 6.95: [HSA] = 1.0×10^{-7} (a), 5.0×10^{-7} (b), 1.0×10^{-6} (c), 2.0×10^{-6} (d) and 4.0×10^{-6} M (e). (B) The same in 0.01 M phosphate buffer pH 4.55: [HSA] = 1.0×10^{-7} (a); 2.0×10^{-7} (b); 5.0×10^{-7} (c); 1.0×10^{-6} (d); 2.0×10^{-6} (e); and 4.0×10^{-6} M (f).

red shift of the absorption spectra is due to higher refractive index of the macromolecular environment compared to that of water. Similar effects were found upon DTC binding to DNA [18] and upon DTC interaction with the interface of normal and reverse micelles [33]. A small CD signal detected for DTC bound to HSA shows very weak asymmetric distortion of the chromophore induced by the chiral protein.

Anionic thiacarbocyanines associate more strongly with HSA than cationic ones (tentatively with partial formation of dye aggregates on HSA), probably, due to their bipolar structure (positive chromophore and negative sulfonate groups) and

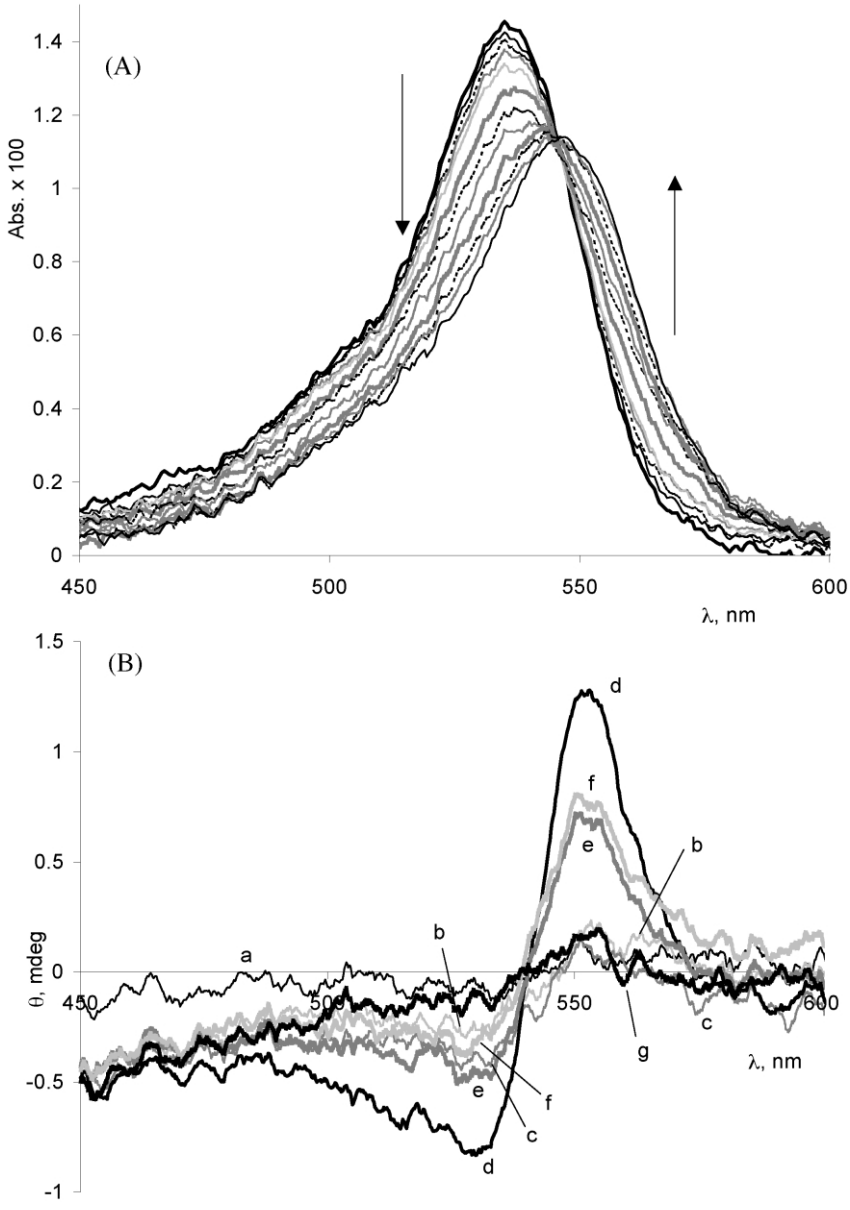

Fig. 8. (A) Absorption spectra of **15** (1.9×10^{-7} M) in water during titration with HSA. [HSA] = 0, 1.95×10^{-8}, 3.86×10^{-8}, 5.75×10^{-8}, 7.61×10^{-8}, 1.23×10^{-7}, 1.71×10^{-7}, 2.18×10^{-7}, 3.11×10^{-7}, 4.04×10^{-7}, 4.96×10^{-7} and 6.78×10^{-7} M. (B) CD spectra of dye **15** (2.2×10^{-6} M) in water in the presence of HSA: [HSA] = 1.0×10^{-7} (a); 2.0×10^{-7} (b); 5.0×10^{-7} (c); 1.0×10^{-6} (d); 2.0×10^{-6} (e); 4.0×10^{-6} (f); and 1.0×10^{-5} M (g).

to the possibility of interaction with both positive and negative charges [27,28] of the protein molecule. More hydrophobic dyes **6** and **7** exhibit larger *K* than **5**; therefore, as for cationic cyanines, both electrostatic and hydrophobic interactions apparently contribute to the binding of the dyes to HSA. Dimers and other aggregates formed by usual cyanines in water decompose in the presence of

HSA, which shows that the forces attaching the dyes to the protein are stronger than those binding dye molecules into their self associates (however, we found that the aggregates of a long-chain squarylium indocyanine dye, bis [1-octadecyl-3,3-dimethylindol-2-ylidene)methyl]squaraine, in water were not split by addition of HSA). We did not find for 7 (which produces J aggregates by itself) any essential stimulation of J aggregate formation by HSA, which was observed for *meso*-tetrakis(*p*-sulfonatophenyl)porphyrin (TSPP) [29]. However, J aggregates appear in the presence of HSA for other anionic thiacarbocyanine, dye **8**, which does not form J aggregates without HSA (Fig. 4).

While dye **5**, unsubstituted in the polymethine chain, is present in solutions (as well as in the complex with HSA) in the form of the all-*trans* isomer, **6** and **7**, having a *meso*-substituent in the polymethine chain, exist in water as the non-fluorescent mono-*cis* isomers [27,28,34]. Binding of **6** and **7** to HSA results in large red shifts of the monomer absorption maxima (33 nm and approx. 40 nm, respectively), much larger than for **5** (10 nm) and appearance of intense fluorescence. Such effects are indicative of *cis*→*trans* conversion and are also observed upon incorporation of **6** and **7** into AOT (sodium bis(2-ethylhexyl)sulfosuccinate) reverse micelles due to strong electrostatic interaction with the interface in the confined micellar environment, giving rise to alignment of charged fragments in the dye molecule along the field [27,28]. The *trans* isomers formed, red-shifted with respect to the corresponding *cis* isomers, are fluorescent; their rigidization in the external electric field raises Φ_f [27,28]. The Φ_f values for **5**–**7** bound to HSA (approx. 0.7 for **5** and **6** and 0.56 for **7**) are similar to those for the dyes incorporated into the relatively small reverse micelles with $w_0 = 0-1$ ($w_0 = [H_2O]/[AOT]$) and much higher than for the dyes in normal micelles (in the latter case the *cis*→*trans* conversion is not complete) [27,28]. Therefore, we may infer that the strength of the electric field created by the charges of the HSA binding sites is similar to that in the reverse micelles, being much larger than in normal micelles.

Asymmetric distortion of thiacarbocyanines (both cationic and anionic) bound to HSA gives rise to appearance of negative CD signals. A negative CD spectrum was also observed for monomeric TSPP complexed with HSA [29]. Larger intensity of CD bands for more hydrophobic dyes **6** and **7** compared to that of **5** shows greater distortion of their molecules and is apparently due to stronger interaction with the chiral protein (higher K) and their bulkier structure. Biphasic (coupled) CD spectra were not detected for **5**–**7**, in spite of tentative aggregate formation on HSA, apparently due to low extinction coefficients of the aggregates.

The peculiarities of the interaction of anionic oxonols with HSA differ substantially from those of thiacarbocyanines. First, Φ_f of **9**–**13** bound to HSA are small in spite of strong complexation with the protein (high K): extremely small for **9**–**11** and **13** and slightly larger for dye **12** with longer polymethine chain. Second, the monomeric CD bands, which appeared upon the complexation, are positive, not negative. The absence of remarkable fluorescence of the bound oxonols might be explained by large free volume within the binding sites of HSA sufficient for free intramolecular motions of dye molecules leading to fast non-radiative deactivation. However, this explanation seems to be unlikely, because the relatively intense CD bands of complexed oxonols indicate rather strong distortion of their molecules in the binding sites, which points to the restricted free volume around the complexed dyes. Furthermore, even much bulkier oxonol **12**, which has to suffer stronger motion restrictions in the binding sites, does not exhibit high Φ_f with HSA. A more likely reason for low Φ_f is the quenching of the excited oxonols by water contained in the protein interior. This could occur by means of hydrogen bonding between excited dyes and water molecules involving negatively charged oxygen atoms of the dyes and can be deduced from a comparison of Φ_f for oxonols in water and in other polar solvents: whereas Φ_f in MeCN, while very small, is measurable (for **9** and **10** Φ_f approx. 10^{-3} [35]), those in water fall down to zero ($<10^{-4}$). Similar fluorescence quenching by water was observed earlier for bis[4-(dimethylamino)phenyl]squaraine,

whose molecule also contains negatively charged oxygen atoms [36]. High association constants K of oxonols could be explained, apart from electrostatic and hydrophobic interactions, by the contribution of hydrogen bonding between dye oxygen atoms and NH groups of the protein. Such bonding has been also found for hypericin—HSA complex, which occurs between the carbonyl oxygen of hypericin and the NH group of the HSA tryptophan residue [37].

Anionic tetracyanopolymethines exhibit lower K than oxonols possibly because they cannot form strong hydrogen bonds with HSA. The quenching of their fluorescence by water is essentially absent (Φ_f for **15** in water and acetonitrile is 0.029 and 0.019 [35], respectively) and an appreciable rise of Φ_f upon complexation with HSA is observed. Even at neutral pH tetracyanopolymethines exhibit partial aggregation on HSA reflected in the characteristic CD spectra. The monomeric tetracyanopolymethines bound to HSA show no CD signal (no chiral deformations), probably due to the relatively small size of their molecules. Growing total positive charge of HSA (by decreasing pH) leads to strengthening electrostatic interactions between HSA surface and oxonols or tetracyanopolymethines, which stimulates strong aggregation of the dyes on HSA. Strengthening hydrophobic interactions (due to an increase in hydrophobicity of the dyes) also stimulates their aggregation on HSA surface. The extensive aggregation is often reflected in the loss of an isosbestic point in the dye absorption spectra (if it was initially present) and appearance of the biphasic CD signal.

In contrast, CD signals were not observed for the dyes incorporated in normal and reverse micelles, which is consistent with achiral framework of the dye molecules in the micelles.

The data obtained do not present enough information on the HSA sites binding polymethine dyes. Small K values found for cationic thiacarbocyanines show that these dyes do not incorporate into high affinity sites of HSA. Weakness of the CD bands observed upon their complexation suggests that the bound dyes are located far from protein chiral centers. Hence, the binding for cationic thiacarbocyanines could occur on the superficial regions of HSA. Anionic thiacarbocyanines (especially more hydrophobic **6** and **7**) exhibit higher K and more intense CD signals, which are consistent with penetration (at least partial) of these dyes into the HSA sites with stronger binding. Anionic oxonols having the highest K and CD bands apparently penetrate into the interior of HSA molecule, namely into the sites of high affinity (probably into two binding sites in the subdomains IIA and IIIA available for complexation of relatively small aromatic or heterocyclic compounds [38]). This could explain the presence of two complexation modes found for dye **9** (see above). The analogous dye **10** interacts only with one binding site of HSA, possibly, due to its larger size.

5. Conclusions

Polymethine dyes bind non-covalently to HSA with various affinity and the association constants ranging from 10^4 to $(5–6)\times10^7$ M^{-1}. Cationic thiacarbocyanines exhibit the lowest K and very weak CD signals, which points to a location of the dyes far from chirality centers and high affinity binding sites (possibly in superficial area of HSA). Anionic thiacarbocyanines with sulfonate groups show much stronger association with HSA (and more intense CD signal), probably, due to their bipolar structure and interaction with both positive and negative charges of HSA. Binding of *meso*-substituted anionic thiacarbocyanines to HSA results in *cis*→*trans* isomerization and, as a consequence, appearance of dye fluorescence. The complete *cis*→*trans* conversion and intense fluorescence of the *trans* isomers formed indicate strong electrostatic field in the corresponding binding sites. Anionic oxonols strongly bind to HSA (due to tentative contribution of hydrogen bonding), showing the highest K and CD bands. The aggregates formed by the dyes alone in aqueous solutions are decomposed in the presence of HSA; the binding to HSA is often accompanied by dye aggregation on HSA, which can exhibit the characteristic excitonic CD spectra.

Acknowledgments

This work was supported by (CQE-4)/FCT (Project POCTI/35398/QUI/2000), by FSE (III

Quadro Comunitário de Apoio) and in part by the Russian Foundation for Basic Research (02-03-32924). Prof. B.I. Shapiro and Dr V.I. Avdeeva are acknowledged for providing anionic thiacarbocyanine dyes and Dr Zh.A. Krasnaya for giving oxonols and tetracyanopolymethines. A.S. Tatikolov thanks FCT for the award of an Invited Scientist Fellowship (BCC/20248/99).

References

[1] S.K. Pal, A. Datta, D. Mandal, K. Bhattacharyya, Photoisomerization of diethyloxadicarbocyanine iodide in micelles, Chem. Phys. Lett. 288 (1998) 793–798.

[2] R. Sabaté, M. Gallardo, A. de la Maza, J. Estelrich, A spectroscopy study of the interaction of pinacyanol with *n*-dodecyltrimethylammonium bromide micelles, Langmuir 17 (2001) 6433–6437.

[3] F. García-Jiménez, M.I. Khramov, R. Sánchez-Obregón, O. Collera, Formation of J-aggregates of cyanine dyes in bilayer lipid vesicles, Chem. Phys. Lett. 331 (2000) 42–46.

[4] N. Nakashima, T. Kunitake, Drastic fluorescence enhancement of cyanine dyes bound to synthetic bilayer membranes. Its high sensitivity to the chemical structure and the physical state of the membrane, J. Am. Chem. Soc. 104 (1982) 4261–4262.

[5] S.P. Velsko, G.R. Fleming, Solvent influence on photochemical isomerizations: photophysics of DODCI, Chem. Phys. 65 (1982) 59–70.

[6] E. Åkesson, V. Sundström, T. Gillbro, Isomerization dynamics in solution described by Kramers' theory with a solvent-dependent activation energy, Chem. Phys. 106 (1986) 269–280.

[7] T.H. James (Ed.), The Theory of the Photographic Process, 4th ed, Macmillan, New York, 1977.

[8] J. Sowell, K.A. Agnew-Heard, J.C. Mason, C. Mama, L. Strekowski, G. Patonay, Use of non-covalent labeling in illustrating ligand binding to human serum albumin via affinity capillary electrophoresis with near-infrared laser induced fluorescence detection, J. Chromatogr. B 755 (2001) 91–99.

[9] R.J. Williams, M. Lipowska, G. Patonay, L. Strekowski, Comparison of covalent and non-covalent labeling with near-infrared dyes for the high-performance liquid chromatographic determination of human serum albumin, Anal. Chem. 65 (1993) 601–605.

[10] R. Philip, A. Penzkofer, W. Bäumler, R.M. Szeimies, C. Abels, Absorption and fluorescence spectroscopic investigation of indocyanine green, J. Photochem. Photobiol. A: Chem. 96 (1996) 137–148.

[11] K. Sauda, T. Imasaka, N. Ishibashi, Determination of protein in human serum by high-performance liquid chromatography with semiconductor laser fluorometric detection, Anal. Chem. 58 (1986) 2649–2653.

[12] E.D. Moody, P.J. Viskari, C.L. Colyera, Non-covalent labeling of human serum albumin with indocyanine green: a study by capillary electrophoresis with diode laser-induced fluorescence detection, J. Chromatogr. B 729 (1999) 55–64.

[13] S. Miki, T. Kaneta, T. Imasaka, Immunoassay for human serum albumin using capillary electrophoresis–semiconductor laser-induced fluorometry, J. Chromatogr. B 759 (2001) 337–342.

[14] I. Timtcheva, V. Maximova, T. Deligeorgiev, N. Gadjev, K.H. Drexhage, I. Petkova, Homodimeric monomethine cyanine dyes as fluorescent probes of biopolymers, J. Photochem. Photobiol. B: Biol. 58 (2000) 130–135.

[15] I. Timtcheva, V. Maximova, T. Deligeorgiev, D. Zaneva, I. Ivanov, New asymmetric monomethine cyanine dyes for nucleic-acid labelling: absorption and fluorescence spectral characteristics, J. Photochem. Photobiol. A: Chem. 130 (2000) 7–11.

[16] S.M. Yarmoluk, D.V. Kryvorotenko, A.O. Balanda, M.Y. Losytskyy, V.B. Kovalska, Proteins and cyanine dyes. 3. Synthesis and spectroscopic studies of benzothiazolo-4-[1,2,6-trimethylpyridinium] monomethine cyanine dyes for fluorescent detection of bovine serum albumin in solution, Dyes Pigm. 51 (2001) 41–49.

[17] M. Kessler, O.S. Wolfbeis, Method for detection and determination of human serum albumin—anionic cyanine dyes, urine analysis. US Patent 5182214, 1993.

[18] M.Y. Anikovsky, A.S. Tatikolov, V.A. Kuzmin, Complex formation between 3,3′-diethylthiacarbocyanine iodide and DNA and its investigation in aqueous solution, Intern. J. Photoenergy 1 (1999) 35–39.

[19] D. Andrews-Wilberforce, G. Patonay, Investigation of near-infrared laser dye albumin complexes, Spectrochim. Acta 46A (1990) 1153–1162.

[20] J.L. Seifert, R.E. Connor, S.A. Kushon, M. Wang, B.A. Armitage, Spontaneous assembly of helical cyanine dye aggregates on DNA nanotemplates, J. Am. Chem. Soc. 121 (1999) 2987–2995.

[21] M. Wang, G.L. Silva, B.A. Armitage, DNA-templated formation of a helical cyanine dye J-aggregate, J. Am. Chem. Soc. 122 (2000) 9977–9986.

[22] I.I. Timcheva, V.A. Maximova, T.G. Deligeorgiev, N.I. Gadjev, R.W. Sabnis, I.G. Ivanov, Fluorescence spectral characteristics of novel asymmetric monomethine cyanine dyes in nucleic acid solutions, FEBS Lett. 405 (1997) 141–144.

[23] N.J.L. Roth, A.C. Craig, Predicted observable fluorescent lifetimes of several cyanines, J. Phys. Chem. 78 (1974) 1154–1155.

[24] J. Arden-Jacob, N.J. Marx, K.H. Drexhage, New fluorescent probes for the red spectral region, J. Fluoresc. 7 (1997) 91S–93S, Supplement.

[25] I. Tinoco Jr, K. Sauer, J.C. Wang, Physical Chemistry: Principles and Applications in Biological Sciences, Prentice-Hall, Inc, Englewood Cliffs, New Jersey, 1978, pp. 454–463.

[26] G. Scatchard, The attractions of proteins for small molecules and ions, Ann. NY Acad. Sci. 51 (1949) 660–672.
[27] A.S. Tatikolov, S.M.B. Costa, Photophysics and photochemistry of hydrophilic cyanine dyes in normal and reverse micelles, Photochem. Photobiol. Sci. 1 (2002) 211–218.
[28] A.S. Tatikolov, S.M.B. Costa, Effects of normal and reverse micellar environment on the spectral properties, isomerization and aggregation of a hydrophilic cyanine dye, Chem. Phys. Lett. 346 (2001) 233–240.
[29] S.M. Andrade, S.M.B. Costa, Spectroscopic studies on the interaction of a water soluble porphyrin and two drug carrier proteins, Biophys. J. 82 (2002) 1607–1619.
[30] M. Dockal, D.C. Carter, F. Rücker, The three recombinant domains of human serum albumin, J. Biol. Chem. 274 (1999) 29303–29310.
[31] G.R. Parr, R.F. Pasternack, The interaction of some water-soluble porphyrins and metalloporphyrins with human serum albumin, Bioinorg. Chem. 7 (1977) 277–282.
[32] Y.V. Il'ichev, J.L. Perry, J.D. Simon, Interaction of ochratoxin A with human serum albumin. Preferential binding of the dianion and pH effects, J. Phys. Chem. B 106 (2002) 452–459.
[33] A.M. Vinogradov, A.S. Tatikolov, S.M.B. Costa, The effect of anionic, cationic and neutral surfactants on the photophysics and isomerization of 3,3′-diethylthiacarbocyanine, Phys. Chem. Chem. Phys. 3 (2001) 4325–4332.
[34] V. Khimenko, A.K. Chibisov, H. Görner, Effects of alkyl substituents in the polymethine chain on the photoprocesses in thiacarbocyanine dyes, J. Phys. Chem. A 101 (1997) 7304–7310.
[35] A.S. Tatikolov, Kh.S. Dzhulibekov, Zh.A. Krasnaya, Fluorescent properties of the polymethine dyes with chromophores in both counter-ions, Izv. AN. Ser. Khim. 1 (1992) 2532–2538, Bull. Russ. Acad. Sci., Div. Chem. Sci.
[36] C.A.T. Laia, S.M.B. Costa, Fluorescence quenching of a squaraine dye by water in AOT reversed micelles, J. Chem. Soc. Faraday Trans. 94 (1998) 2367–2373.
[37] P. Miskovsky, D. Jancura, S. Sánchez-Cortés, E. Kocisova, D. Jancura, L. Chinsky, Antiretrovirally active drug hypericin binds the IIA subdomain of human serum albumin: resonance Raman and surface-enhanced Raman spectroscopy study, J. Am. Chem. Soc. 120 (1998) 6374–6379.
[38] X.M. He, D.C. Carter, Atomic structure and chemistry of human serum albumin, Nature 358 (1992) 209–215.